

Study on Critical Micelle Concentration Influence in Green Synthesis of Silver Nanoparticles Assisted by *Sapindus mukorossi* Aqueous Extract

RADU LUCIAN OLTEANU¹, CRISTINA MIHAELA NICOLESCU¹, MARIUS BUMBAC^{2*}, IOANA DANIELA DULAMA¹,
RODICA MARIANA ION^{3,4}, IOANA RALUCA SUICA BUNGHEZ¹

¹Valahia University of Targoviste, Institute of Multidisciplinary Research for Science and Technology, 18-24 Unirii Blvd., 130082, Targoviste, Romania

²Valahia University of Targoviste, Faculty of Sciences and Arts, Sciences and Advanced Technologies Department, 18-24 Unirii Blvd., 130082, Targoviste, Romania

³Valahia University of Targoviste, Faculty of Materials Engineering and Mechanics, Materials Engineering Department, 18-24 Unirii Blvd., 130082, Targoviste, Romania

⁴National Research and Development Institute for Chemistry and Petrochemistry -ICECHIM, 202 Splaiul Independentei, 060021, Bucharest, Romania

Silver nanoparticles synthesis mediated by plant extracts involves the colloidal stability of generated metallic particles in solutions. Formation of micelles in solutions influences the nanoparticle synthesis process and consequently, the surface plasmonic response (SPR) of the formed silver nanoparticles. Critical micelle concentration (CMC) of Sapindus mukorossi aqueous extract has been determined with ultraviolet-visible spectroscopy, two methods were used: dye micellization method, and correlation of silver nanoparticles SPR with the variation of surfactant concentration. Results obtained for CMC determination by the two methods were highly reproducible and in good correlation indicating that micelles formed by saponins present in the Sapindus mukorossi aqueous extract are useful as effective structure-driving agents to synthesize colloidal metallic nanoparticles, offering them proper growth conditions. Silver nanoparticles synthesis mixtures were studied, with Sapindus mukorossi aqueous extract and silver nitrates as precursors, in acidic and basic media, at room temperature to establish correlations between saponins structure modifications and surface plasmonic response of metallic nanoparticles. Light absorption spectrometric techniques (ultraviolet-visible and infrared), X-ray diffraction and scanning electron microscopy were used to characterize the synthesis process.

Keywords: critical micelle concentration, *Sapindus mukorossi*, silver nanoparticles green synthesis

Saponins derived from natural renewable sources have a potential use as surfactants due to their high degree of biocompatibility and biodegradability. Studies on their physico-chemical characterization (either in mixtures, or as individual components) have been reported [1-3]. The fruit pericarp of trees from *Sapindaceae* family is widely used as natural detergent and its extract is commercially used as foam stabilizing and emulsifying agent in cleansers, shampoos, and cosmetics; the reason is that pericarp is abundant in saponins, mostly of triterpenoid-type with high surface activity [4].

Surfactants are amphiphilic substances consisting in a long-chain hydrocarbon *tail* and a polar *head*. A unique property of surfactants is that, their molecules arrange themselves into organized molecular aggregates, known as micelles if the concentration exceeds a specific value, called critical micelle concentration (CMC) [5].

The value of critical micelle concentration can be correlated with the changes in physico-chemical properties of the surfactant solution. The micelles forming property is affected by temperature, salt concentration and pH of the aqueous phase [6, 7]. It was experimentally demonstrated that CMC value increases with temperature and pH, and is lowered by increased salt concentrations [8]. With regards to size of saponins micelles, it was found that temperature has a significant influence. Increase of temperature lead to higher dimensions of micelles, while salt concentration and pH have a weak influence in this respect [7]. Among the solution physico-chemical properties that may have influence on CMC specific value, solution detergency,

viscosity, density, conductivity, surface tension, osmotic pressure, interfacial tension, refractive index, and light scattering have been reported. However, depending on the methods used to study the behavior of bulk solutions containing surfactants, some differences are observable in values of CMC obtained for the same surfactant. It was generally accepted that the critical micelle concentration is not a precisely defined value, but a range of concentrations at which micelles are formed [9, 10].

Common spectroscopic methods for determining aqueous critical micelle concentration make use of additives whose change in ultraviolet-visible absorbance or fluorescence emission indicate the onset of micelle formation. In a typical setup, a constant amount of organic dye is solubilized in solutions while increasing the amount of surfactant added to solution. Changes of absorption or emission is plotted against the surfactant concentration, and, the inflection point of sigmoidal curve obtained is taken to be the critical micelles concentration [5]. In an ideal case, the amount of solubilized substance varies linearly with the surfactant concentration above the CMC. Other experiments using this method, as well as techniques using stable silver nanoparticles solutions have been described recently [12-14, 25]. However, these methods generally referred to chemical synthetic surfactants, and when plant derived surfactants were studied, previous steps of separation and/or isolation were applied prior to CMC determination.

The increased use of nanoparticles recorded in the last years lead to an important development of knowledge

* email: m_bumbac@yahoo.co.uk; Phone +40-245213382

related to synthesis process. Metallic nanoparticles are prepared in aqueous or non-aqueous solutions by reducing metal ions (added in the reaction medium as metallic salt) with a reductive agent. A significant variety of plant extracts were studied to grow silver nanoparticles, the aggregation behavior of the formed particles being related with the reductive and stabilizing capacity of their organic constituents [15,16].

In present study, an original experimental setup was used for critical micelles concentration determination by correlating the changes of the optical properties (specifically of the SPR) of solutions containing silver nanoparticles synthesized using raw *Sapindus mukorossi* aqueous extract. Silver nitrate was used as silver ions source for the synthesis. An adapted dye micellization method [13] was applied to compare and validate obtained values. Also, the potential influence of micelle formation, and corresponding CMC values, on silver nanoparticles synthesis process was studied, for different compositions of synthesis mixtures, acid and alkaline. Reactants and reaction products were characterized by light absorption spectroscopy (infrared (IR), ultraviolet - visible (UV-Vis)), X-ray diffraction (XRD) and scanning electron microscopy (SEM), and conclusions about the role of critical micelles concentration on silver nanoparticles synthesis were drawn.

All experiments were conducted in aqueous media that was considered the best choice in terms of efficiency of saponins extraction, comparing with use of organic solvents. Also for potential large-scale applications, environmental and cost efficiency are significantly better for the use of water as solvent [1,11].

Experimental part

Materials and methods

The plant aqueous extract was obtained using dried *Sapindus mukorossi* soapnut shells of Indian origin, purchased from a local authorized supplier (EcoNat); raw product of same batch was used during tests. Silver nitrate (crystalline, 99.80% purity), potassium hydroxide (pellets, 85 - 100 %, < 1 % carbonate) and methylene blue (dye content > 82 %, spectrophotometrically) reagents, for analysis purity, were purchased from Merck Millipore; all other solvents and chemicals were of analytical grade from Chimopar SA. Redistilled water (conductivity at 25°C below 0.5 $\mu\text{S}\cdot\text{cm}^{-1}$) was used for extraction, determination of CMC, nanoparticles synthesis and for other analytical methods applied during experiments.

The pH of solutions was measured with Inolab Multi 9430 meter using IDS SenTix 980 pH-sensor, with an accuracy of $4\cdot 10^{-3}$ pH units. Centrifugation was performed with a Rotofix 46 Hettich Lab Technology centrifuge, at a speed of 1000 rpm.

Spectroscopic measurements were performed on the ultraviolet-visible double beam Evolution-260BIO spectrophotometer (Thermo Scientific), using quartz cuvettes of 1 cm as sample support.

Sapindus mukorossi extract preparation

Air-dried, powdered soapnut shells (30 g) were mixed with redistilled water (300 mL) for 6 hours under magnetic stirring, at room temperature. After centrifugation at 1000 rpm for 10 minutes and the resulted extract was filtered (Whatmann no. 4). This extract stock solution was stored at 4°C for further tests.

Critical micelle concentration (CMC) determination

CMC was evaluated by two experimental procedures performed at room temperature, obtained values were

compared. First method was based on dye micellization procedure [12, 13], and the second one used the surface plasmon response characteristic of metallic nanoparticles [14-16, 25]. All these experiments used raw soapnuts extract, without previous isolation of saponins.

The method proposed by Patist et al. [13], adapted for the working conditions, was applied to calculate the critical micelle concentration of soapnuts extract by using methylene blue (methylthioninium chloride) dye, aqueous solution with concentration of 10^{-4} M. A series of test samples were prepared by adding different aliquots of extract stock solution ($100\div 1000$ μL), each in a 25 mL volumetric flask where a volume of 2.5 mL of methylene blue 10^{-4}M was previously pipetted, then filled to the mark with redistilled water. For the spectroscopic measurements, individual reagent blank solutions for tested samples were used; these were prepared in the same manner as samples, but without soapnuts extract, redistilled water was added instead. Visible spectra of samples were recorded in the wavelength range of 500-800 nm, at 1 nm intervals, versus the reagent blank prepared as above. For all the scanned solutions, the wavelength corresponding to the absorption maxima λ_{max} were read and centralized. These values were then plotted versus the extract concentration in studied samples. The CMC was calculated as the value corresponding to the crossing point of the two linear tendency segments of the graph.

For CMC determination using the SPR of nanoparticles, mixtures of soapnuts extract and a stable silver nanoparticles colloidal solution were used, according to an adapted method described in the literature [14]. Choice of the stable silver nanoparticles solution was done according to previous studies [15, 16]. Tests were performed at room temperature, samples absorbances at the fixed wavelength of 418 nm were recorded. This value corresponds to the maximum absorbance recorded for the chosen stable nanoparticles solution. First sample was prepared by adding an aliquot of 50 μL from *Sapindus mukorossi* extract stock solution to 10 mL silver nanoparticles stable solution. Absorbance of this mixture was read at 418 nm, over a blank prepared the same way, but with redistilled water instead of nanoparticles solution. Incremental addition of 50 μL aliquots was used to prepare next samples and corresponding individual blanks, and absorbance was measured after each addition. In the end, recorded absorbance values were plotted versus the extract concentration in studied samples, and CMC was determined as the value corresponding to the inflection point graphically identified.

Silver nanoparticles synthesis

Silver nanoparticles were obtained by mixing *Sapindus mukorossi* extract stock solution with silver nitrate (10 mM) solution in different proportions. Synthesis experiments were done in acidic and alkaline media. The acidity of solutions resulted after mixing the nanoparticles precursors was considered appropriate for the study ($\text{pH} = 4.4$), no other pH buffer was added. The pH adjustment for alkaline media was obtained by adding 1 M potassium hydroxide solution to all alkalized samples, up to a pH value around 8.2). Total volume of all tested solutions was 50 mL, and redistilled water was used for necessary dilutions. The mixing order of samples constituents was: dilution water, potassium hydroxide solution (where the case), soapnuts extract, and, after a waiting time of 20 min, the silver nitrate solution. During experiments, mixtures were kept in dark, at room temperature, except the short periods of UV-Vis spectra recording.

Ultraviolet - visible spectroscopy

Spectroscopic study of the colloidal solutions containing nanoparticles prepared during experiments was realized by recording corresponding spectra in the range 230 – 750 nm, at 1 nm intervals. Triplicate synthesis samples were tested, at different mixing ratios of precursors (silver nitrate and soapnuts aqueous extract). Spectra were recorded for each sample *versus* a blank prepared in the same manner, but without silver nitrate.

Infrared (IR) spectroscopy

The infrared spectra were recorded for the soapnut shells extract samples and synthesis mixtures on Fourier Transform Infrared Spectrometer Vertex V80 (Bruker) in the wavenumber range of 4000 cm^{-1} to 400 cm^{-1} . Prior to scanning, samples were placed in glass Petri dishes and dried in oven at 30°C for 24 hours. The use of infrared spectroscopy data aimed to identify structural changes that may suggest the nature of interactions of soapnut extract components and silver nanoparticles synthesized.

X-ray Diffraction / XRD

Present study used X-ray diffraction technique to characterize the nanoparticles synthesized using *Sapindus mukorossi* aqueous extract and silver ionic solution. Samples were prepared by mixing the plant extract, prepared as described above, with 10 mM silver nitrate solution in five different proportions: 1:1, 1:2, 1:4, 2:1 and 4:1. The mixtures were kept for three hours in dark, at room temperature, then samples were evaporated to dryness in a lab circulation oven, at 30 °C. The solid matter was analyzed by X-ray diffraction using a Rigaku Ultima IV instrument, equipped with Cu K α ($\lambda = 1.54056 \text{ \AA}$) radiation source, set at 40 kV and 20 mA. Powder diffraction patterns were recorded for dried plant synthesis mixtures and blank (dried plant extract). The geometry used was parallel beam, in continuous scan mode at 1 deg./min. speed and 0.02 deg. step width, in the 2-theta range of 5 - 80 deg.

Scanning electronic microscopy

Scanning electronic microscopy (SEM) was used to characterize the size, shape and morphology of the synthesized silver nanoparticles. A microscope Hitachi SU-70 with field emission was used, with a resolution of 1 nm at 15 kV acceleration voltage. Samples of colloidal silver nanoparticles were placed on aluminium stubs, dried for 30 min at 40°C in a laboratory oven, and then measured at different magnification orders and 25 kV acceleration voltage [21-24].

Results and discussions

Evaluation of critical micelles concentration using dye micellization method

For dye micellization experiments, methylene blue (methylthionium chloride) was chosen because it has a relative narrow absorption maximum (λ_{max}) around 670 nm in aqueous solutions [19, 20]. Thus, when mixing methylene blue solution with studied surfactant the shifts of the wavelength corresponding to maximum absorbance could be easily noticed when surfactant content was modified. The dye significantly changes its ultraviolet - visible response, once the micelles are formed, specifically when surfactant concentration exceeds CMC. Following the association of surfactant molecules as micelles, the ultraviolet - visible spectrum shows a significant shift of the absorption maximum when CMC is reached [13].

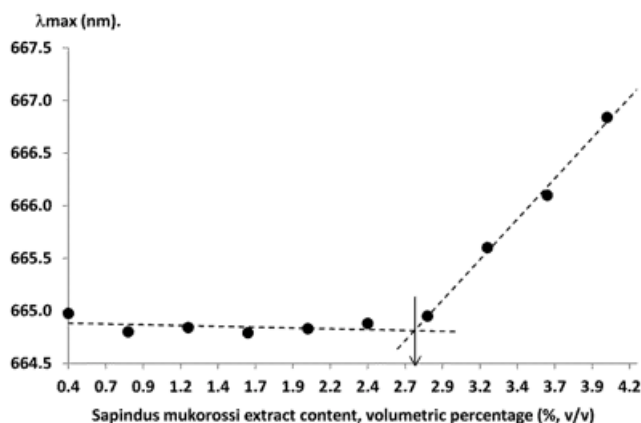


Fig. 1. Critical micelle concentration determination of *Sapindus mukorossi* extract using dye micellization method

The micelles presence in the aqueous extract of *Sapindus mukorossi* was correlated with changes in ultraviolet - visible spectrum of methylene blue added to the mixture. The wavelength values for the maximum absorption recorded as described in the experimental section were plotted versus *Sapindus mukorossi* extract content of studied solutions, as shown in figure 1. Two distinct linear segments were noticed, a slow increase of the λ_{max} , the wavelength corresponding to absorption maxima, was recorded as seen in the first region, followed by a second linear segment with a sudden increase of the wavelength represented on Y axis. Micelles formation is associated with the rapid increase of the λ_{max} . The CMC was calculated as the corresponding X axis value for the crossing point of the tendency line of the two linear segments, obtained value was $2.71 \pm 0.11 \%$.

Correlation of surface plasmonic response (SPR) of silver nanoparticles with the critical micelles concentration (CMC)

Salem et al. [14] reported the use of spectral shift of SPR bands for N-cetyl-N, N, N- trimethylammonium bromide, hydroxyethyl laurdimonium chloride, and N-cetylpyridinium bromide monohydrate to set the value of CMC. In another paper, Karimi et al. [25] showed that the absorption intensity at a fixed wavelength for sodium dodecyl sulfate and trimethyl ammonium bromide changes radically when the surfactant concentration increases over CMC value. Considering these references, an adapted method was developed and applied in present study. The CMC of *Sapindus mukorossi* extract was determined using silver nanoparticles solutions. By plotting

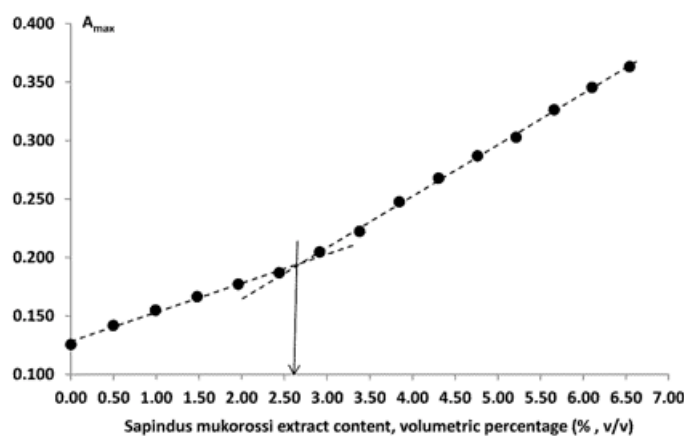


Fig. 2. Critical micelle concentration determination of *Sapindus mukorossi* extract using SPR band sensitivity of a stable silver nanoparticles solution (418 nm)

maximum absorbance (A_{max}) versus *Sapindus mukorossi* extract content in test solution, CMC was determined using linear regression (fig. 2) as 2.68 ± 0.13 %, v/v.

The determined CMC of aqueous *Sapindus mukorossi* extract by the two described spectroscopic methods showed good correlation (2.71 ± 0.11 %, v/v and 2.68 ± 0.13 %, v/v respectively).

Micelles formation and surface plasmonic response of silver nanoparticles synthesized with Sapindus mukorossi extract involves the colloidal stability of the metallic particles in solution. Therefore, the formation of micellar surfactants in the mixture may influence the formation equilibrium of metallic nanoparticles. Consequently, the plasmonic response of the silver nanoparticles formed in solutions having mixtures with different initial volumetric ratios *Sapindus mukorossi* extract: silver nitrate was examined. The CMC value taken as a reference for the micelles presence in the synthesis solutions, where silver nanoparticles are formed, was found to be approximately 2.7 %, according to results described above.

Metallic nanoparticles synthesis by bottom-up approach involves two main processes, the reduction of metallic ion and colloidal stabilization of the particles formed in solution. The freshly formed small dimension particles coalesce due to their low colloidal stability to form larger nanoparticles with different shapes and sizes until they reach a stable form, interfacial force being the main interaction that controls this process. Usually organic compounds, such as surfactants, polymers and stabilizing ligands, are used to passivate the particles to prevent them from further aggregation, the choice of protective agent being one of the most important factors in nanoparticles synthesis [26].

The change of micelle structures has an energetic barrier as May and Ben-Shaul reported [27]. It was found that at low surfactant concentrations, spherical micelles appear in solution. When the surfactant concentration in solution reaches a well-defined saturation value, the energetic barrier is overcome and the micelle structure changes from spherical micelles to other structures, and the micelles will have new stable forms in another concentration range. The special micelles are useful as effective structure - driving agents to prepare nanoparticles with desired morphologies [26]. Thus, the micelle formed by the surfactant with a certain favorable concentration can offer appropriate growth conditions for nanoparticles.

The size and distribution of silver nanoparticles is an outcome of different kinetics of all the stages involved in the nanoparticles formation process. Result of this influence is reflected in the shape of absorption band in the region 350 - 600 nm, cumulating plasmonic properties of all silver nanoparticles in solution [28]. In present study, the surface plasmon response of the particles was followed by recording the UV-Vis spectra of the synthesis mixtures containing plant extract and silver nitrate as precursors.

Figure 3 is presents the UV-Vis spectra for solutions containing silver nanoparticles prepared by adding *Sapindus mukorossi* extract and silver nitrate 10 mM solution with 1:1 volumetric ratio. The inset of the graph presents corresponding relative areas versus volumetric content of *Sapindus mukorossi* extract, calculated for 3 days spectra.

The sample blank solutions (diluted plant extract solutions) and the samples containing silver nitrate had pH values around 4.4, this behavior showing that the extract has buffering properties. The pH value is consistent with the saponins structure, of weak acidic species, reported to be present in the aqueous extract of *Sapindus mukorossi* [29].

It was observed that, in these conditions, formation of nanoparticles is a very slow process, notable changes both in color of colloidal solutions (colorless to light pink and reddish) and ultraviolet - visible spectra were observed at three days from the mixing moment.

Relative areas calculated as the area under the absorption band recorded for samples relative to blank extract solutions in the 350 - 600 nm wavelength domain were correlated with the existence and growth of silver nanoparticles. Relative area vs. plant extract volumetric content plots was preferred to plot of the maximum absorption vs. extract content, because absorption bands had different characteristics (maximum intensity, bandwidth, shape) when different volumetric contents of plant extract were used. The calculation wavelength range has been selected as it is the area of spectra comprising main silver nanoparticles plasmonic properties modifications [28].

The plots represented in figure 3 showed broad absorption bands centered at about 450 nm for all studied samples when they are recorded after three days after the initial mixing moment of the extract stock and silver nitrate solutions. It was observed that, when the volumetric percentage of plant extract solutions exceeds the value of 2.6 ± 0.10 % (fig. 3) the absorbance of the nanoparticles

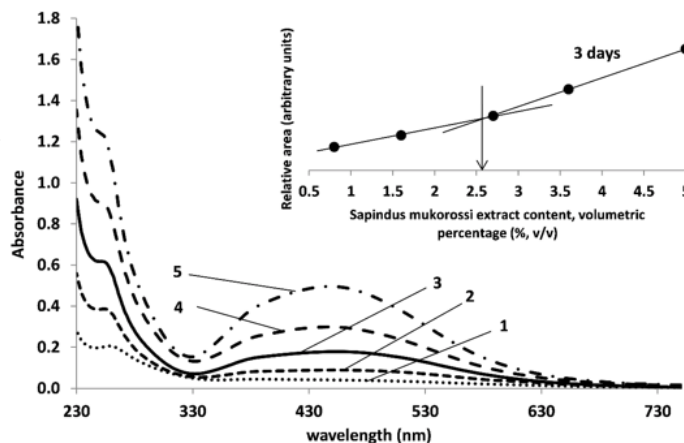


Fig. 3. UV-VIS spectra after 3 days, in acidic media (pH = 4.4), for samples with initial volumetric ratio *Sapindus mukorossi* extract : silver nitrate of 1 : 1, for different extract concentrations (% , v/v): line 1) 0.8 %; line 2) 1.6 %; line 3) 2.7 %; line 4) 3.6 %; line 5) 5 %.

solution increases suddenly. The volumetric content of 2.6 % is confirmed by inflection point value of the graph confirming the assumption that micelles may become driving structures for nanoparticles formation.

Some reported studies showed that micelles may control the rate of synthesis, size, and the shape of metal nanoparticles because surfactant is in dynamic equilibrium with its components (surfactant monomers, micellar aggregates and monomers absorbed as a film at the interface). Surfactant micelles surrounding the colloidal particles also may solubilize and control the orientation of substrates, hydrophobic and hydrogen bonding being responsible for controlling the orientation of silver ions into the Stern layer of micellar pseudo-phase. The micelle can be seen like as porous clusters with aqueous cavities where silver ions are reduced to form metallic particles [30]. Also, the stability, shape, size, and morphologies of metal nanoparticles depend on the method of concentration of stabilizers [31- 33].

UV-Vis spectra for silver nanoparticles colloidal solutions obtained at alkaline pH have been recorded during experiments, figures 4 and 5 respectively show the data measured at three hours and three days respectively, counted from the moment of precursors mixing. The inset

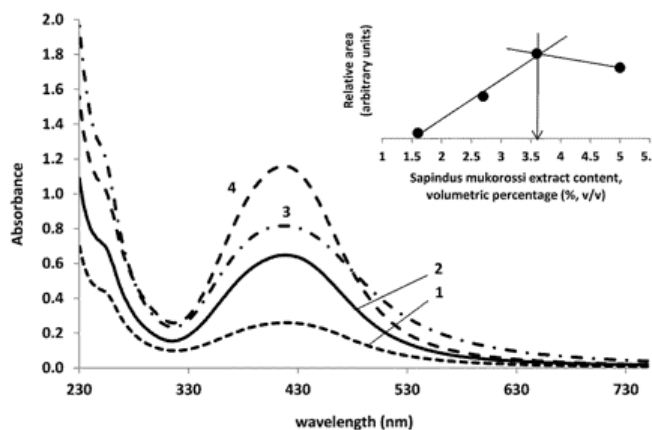


Fig. 4. UV-Vis spectra at 3 hours from mixing, in alkaline media ($\text{pH} = 8.2$), for samples with initial volumetric ratio *Sapindus mukorossi* extract : silver nitrate of 1 : 1, for different extract concentrations (% , v/v): line 1) 1.6 %; line 2) 2.7 %; line 3) 3.6 %; line 4) 5 %.

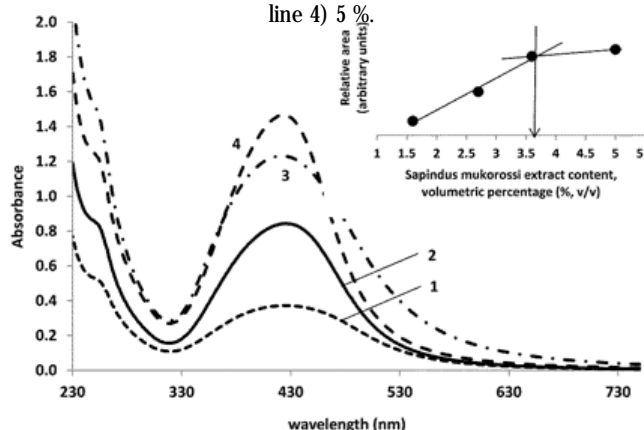


Fig. 5. UV-Vis spectra at 3 days from mixing, in alkaline media ($\text{pH} = 8.2$), for samples with initial volumetric ratio *Sapindus mukorossi* extract : silver nitrate of 1 : 1, for different extract concentrations (% , v/v): line 1) 1.6 %; line 2) 2.7 %; line 3) 3.6 %; line 4) 5 %.

within each corresponding graph presents the calculated relative areas versus volumetric content of *Sapindus mukorossi* extract. UV-Vis for alkalinized samples had higher absorbances and lower peak width values corresponding to the SPR compared with the acidic samples. This was correlated with a successful formation of nanoparticles, more rapid in alkaline media than in acidic ones. For alkaline samples, maximum absorbance peaks were centered on 419 nm after three hours from mixing start (figure 4), while slightly red-shifted peaks centered on 425 nm can be observed in figure 5, for spectra recorded at three days.

Values of CMC in alkaline media, determined as shown in the insets of figures 4 and 5, showed similar values, 3.65 ± 0.19 % for 3 hours, and 3.68 ± 0.12 % for 3 days. The inflection points in the plots relative areas versus extract concentration was assigned to increase of CMC values. Chemical species contained by the aqueous extract have a weak acid character. It was considered that once the alkaline solution is added, deprotonation of acid functional groups occurs, and a mixture of compounds having a weaker hydrophobic character may form. Consequently, this decrease in the hydrophobic character of studied solutions could lead to higher values of CMC. Data presented in figures 4 and 5 shows that CMC has a significant influence on the formation degree of silver nanoparticles in studied synthesis conditions.

The possible functional groups responsible for silver nanoparticles stabilization were studied by Fourier

transform infrared spectroscopy (FT-IR). Some recent studies in this area pointed out that saponins are clearly detectable in the crude aqueous and alcoholic soapnut extracts even before the purification of saponins directly using FT-IR spectroscopy, therefore shortening the time and the necessity for purification steps before performing

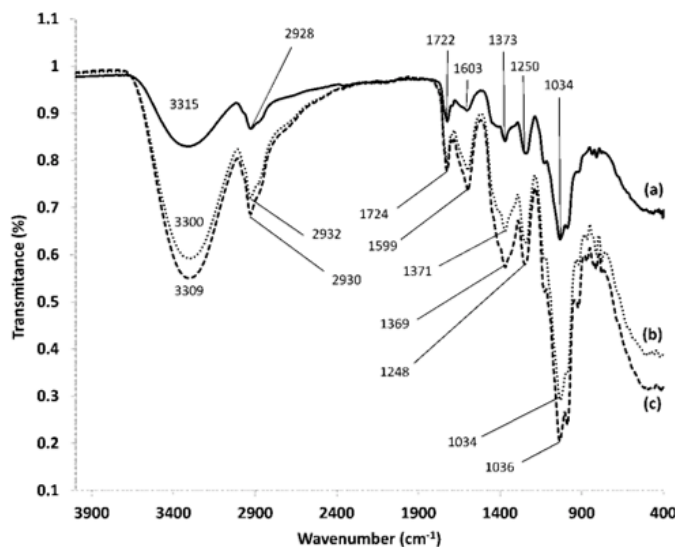


Fig. 6. FT-IR spectra of *Sapindus mukorossi* extract line a) and the soapnut mediated silver nanoparticles at different volumetric ratio mixture soapnut shells extract : silver nitrate solution 10 mM line b) 2:1 and line c) 1:1, ($\text{pH} = 4.4$).

analysis [34, 35]. The FT-IR spectra of *Sapindus mukorossi* extract and soapnut shells mediated silver nanoparticles are shown in figure 6.

The FT-IR profiles of soapnut shells extract and silver nanoparticles synthesized revealed that biomolecules have functional groups specific to saponins and flavonoids that might play an important role in the stabilization of silver nanoparticles during the synthesis process [36]. The FT-IR spectra of soapnut shells (fig. 6-a) shows the presence of transmittance peaks at 3315, 2928, 1722, 1603, 1373, 1250, and 1034 cm^{-1} . The first two peaks are specific to O-H stretching vibration of bounded and unbounded O-H [34 - 37]. The peaks at 1722, 1603, and 1373 cm^{-1} are characteristic of C-O stretching vibration [4, 6, 34], C=C bond [34], and O-H bending vibration, respectively. In addition, the transmittance peak at 1250 cm^{-1} indicates the C-O stretching vibration [36], and transmittance peak from 1034 cm^{-1} can be due to existence of C-O-C [35] and carboxylic ester [4]. The peaks at 4 2928 and 1373 cm^{-1} indicate also the presence of CH_2 groups [4]. This finding indicates the possible presence of carboxylic groups, which is in good agreement with the pH value of the extract solution.

The FT-IR spectra of the soapnut shells mediated silver nanoparticles (fig. 6a and c) showed some shifts corresponding to the stretching vibration of O-H bond at 2930 and 2932 cm^{-1} [36], the stretching vibration of C-O from 41600 cm^{-1} [36] and 41724 cm^{-1} [4], and the stretching vibration of C-O bond at 1248 cm^{-1} [36]. These observations may suggest that the resulting silver nanoparticles might be stabilized by functional groups present in the biomolecules of soapnut shells extract such as saponins and flavonoids through the interactions of carboxylic groups in the saponins as well as the carbonyl groups in the flavonoids [36, 37].

Figure 7 shows a comparison between XRD patterns recorded for the plant extract, and for silver nitrate-plant extract synthesis samples, prepared according to procedure described in the experimental section.

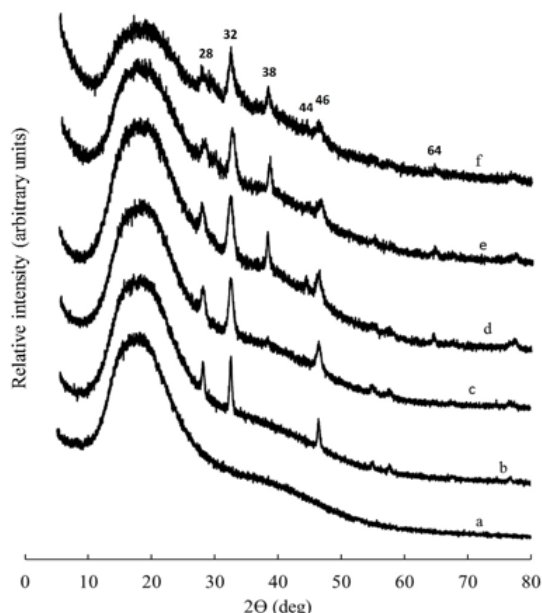


Fig. 7. Comparative graph with X-ray patterns recorded for: line a) plant extract, and synthesis samples with initial volumetric ratio plant extract : silver nitrate of: line b) 4 : 1, line c) 2 : 1, line d) 1 : 1, line e) 1 : 2, line f) 1 : 4, (plant extract % = 2.7 %, pH = 4.4)

Comparative evaluation of samples structure and composition has been performed. For blank samples, the recorded diffractogram showed a high broad peak in the 2θ range of $10\text{--}25^\circ$, with no narrow peaks, suggesting the amorphous character of the dried aqueous plant extract. For samples prepared with silver nitrate and plant extract, the intensity of the amorphous peak decreases with the volume of extract added to the initial mixture, and new narrow peaks appear suggesting formation of crystalline compounds during the synthesis process. Mutual existence of crystalline and amorphous phases in samples after synthesis may suggest that some plant constituents remain attached to the formed particles. Consistency with infrared and ultraviolet-visible absorption spectroscopy studies described above could be found.

Figure 7 (lines b - f) shows that for all the samples where the initial mixture contained silver nitrate, recorded diffractograms present peaks at 2θ values around $28, 32$

and 46° . Comparing these values with data from ICDD diffraction cards 01-074-4790, presence of silver nitrate may be suggested. Also, the 2θ peak from 46° decrease in intensity with the increase of silver nitrate content in the initial mixture. In the same time, for volumetric ratio plant extract: silver nitrate 10 mM solution in the initial mixtures of 1:1 (line d), other peaks appear at 2θ values of $38, 44$ and 64 degrees, that suggest presence of metallic centrosymmetric silver (ICDD card 04-003-7118). Table 1 presents experimental and standard diffraction data for silver identified as existing crystalline phase in studied mixtures; corresponding diffraction angles, interplanar spaces and Miller indices are included for the most significant three peaks. Intensities of the peak at 2θ angle of 38° were compared for the studied samples. It was observed that the highest value was recorded for samples with initial mixing ratio plant extract: silver nitrate of 1:1 (line d), while the intensity of this peak decreases for samples with 1:2 (line e) and 1:4 (line f) volumetric ratios, respectively. Also, this peak was slightly visible for samples with initial 2:1 (line c) plant extract: silver nitrate ratio, and did not appear when the ratio was 4:1 (line b).

The XRD study confirms presence of crystalline silver in studied samples, mainly in the samples where the initial mixing ratio plant extract: silver nitrate used for synthesis is 1:1 or lower. Presence of non-reacted silver nitrate was also confirmed in synthesis samples through X-ray diffraction. With regards to silver presence in samples after synthesis, table 1 shows a good agreement between experimental and standard diffraction data, for an initial mixing ratio 1:1.

As reported in other studies, the XRD setup used proved to offer valuable experimental information on nanoparticles identification and also on samples crystallinity evolution related to certain control samples. [38, 39]

Figure 8 shows images obtained by SEM for samples prepared with different concentrations of plant extract. It was observed that when higher concentrations of extract were used in the initial mixture particle, conglomerates were formed. Particles formed were spherical as shape in all cases. At higher extract concentration, larger conglomerates appear and decrease of the nanoparticles content was registered.

Table 1
EXPERIMENTAL AND STANDARD DIFFRACTION DATA FOR SILVER, FOR SAMPLE WITH INITIAL MIXING RATIO PLANT EXTRACT : SILVER NITRATE OF 1 : 1.

Experimental data		Standard data (ICDD card 04-003-7118)		Miller Indices (h, k, l)
Diffraction angle, 2θ , (degrees)	Interplanar spacing, d, (Å)	Diffraction angle, 2θ , (degrees)	Interplanar spacing, d, (Å)	
38.02 ± 0.03	2.3647 ± 0.0016	37.9803	2.367140	(1, 1, 1)
44.15 ± 0.08	2.049 ± 0.004	44.1409	2.050000	(2, 0, 0)
64.28 ± 0.14	1.448 ± 0.003	64.1982	1.449570	(2, 2, 0)

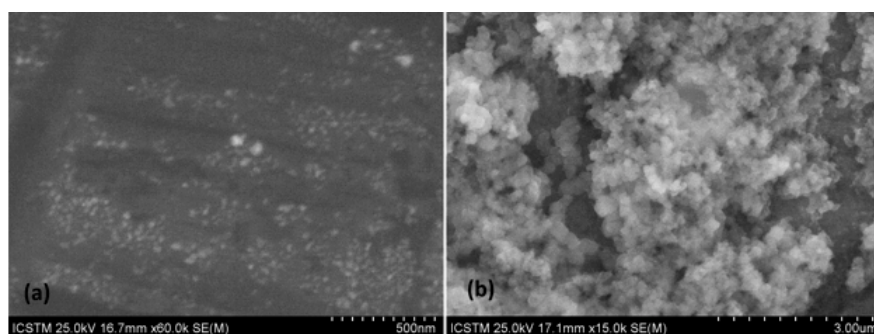


Fig. 8. Scanning electron microscopy images for samples with initial mixing ratio soapnuts extract : silver nitrate 10 mM of 1 : 1, at initial extract content(v/v) of 0.8% (a), and 2.7 % (b)

Conclusions

Sapindus mukorossi is a species of tree in the *Sapindaceae* family with fruits commonly known as Indian Soapberry. The extract of *Sapindus mukorossi* contains saponins and therefore its aqueous extract behaves as surfactant solution.

Critical micelle concentration is an important parameter for surfactants characterization, its value indicating the influence of surfactant concentration on the micellar stabilization process. The critical micelle concentration (CMC) of aqueous *Sapindus mukorossi* extract was determined by dye micellization method, and by correlation of surface plasmonic response of silver nanoparticles with the variation of surfactant concentration. The two methods showed high reproducible and well correlated results, 2.71 ± 0.11 (% v/v) and 2.68 ± 0.13 % v/v respectively. These data indicate that micelles formation are structuring driving agents for the formation of silver nanoparticles.

The formation of micelles in the mixture influences the nanoparticle synthesis process and consequently, the plasmonic response of the silver nanoparticles formed in solutions. *Sapindus mukorossi* aqueous extract had acidic pH indicating the presence of weak acidic species in the mixture. Plant extract alkalization lead to deprotonation of acidic functional groups from the saponins structure present in the *Sapindus mukorossi* extract. Therefore, the structure, shape, and size of micelles changes and, consequently, the value of CMC changes also. In basic conditions, the graphical representation of the relative areas calculated from the UV - Vis spectrum, for the wavelength domain 350 - 600 nm, presented an inflection point at CMC values of 3.65 ± 0.19 % after 3 h, and 3.68 ± 0.12 % after 3 days from mixing moment of plant extract and silver nitrate. This behavior was assigned to the hydrophobicity decrease of the weak acid species from the extract solution due to deprotonation in the basic medium.

The X-ray diffraction study, presence of crystalline silver in samples after synthesis was confirmed, experimental data being in good correlation with standard diffraction data for silver. SEM images and FTIR spectra confirmed also that silver nanoparticles are formed in the samples obtained by mixing silver nitrate with *Sapindus mukorossi* extract.

References

1. ROY, D., KOMMALAPATI, R.R., MANDAVA, S.S., VALSARAJ, K.T., CONSTANT, W.D., Environ. Sci. Technol., **31**, 1997, p. 670
2. MUNTAHA, S.-T., KHAN, M.N., J. Cleaner Prod., **93**, 2015, p. 145
3. PEIXOTO, M.P.G., TRETER, J., DE RESENDE, P.E., DA SILVEIRA, N.P., ORTEGA, G.G., LAWRENCE, M.J., DREISS, C.A., J. Pharm. Sci., **100**, no. 2, 2011, p. 636
4. LI, R., WU, Z.L., WANG, Y.J., LI, L.L., Ind. Crops Prod., **51**, 2013, p. 163
5. FURTON, K.G., NORELUS, A., J. Chem. Edu., **70**, no. 3, 1993, p. 254
6. NEGI, J.S., NEGI, P.S., PANT, G.J., RAWAT, M.S.M., NEGI, S.K., J. Poisonous Med. Plant Res., **1**, no. 1, 2013, p. 001
7. MITRA, S., DUNGAN, S.R., J. Agric. Food Chem., **45**, no. 5, 1997, p. 1587
8. BALAKRISHNAN, S., VARUGHESE, S., DESHPANDE, A.P., Tenside Surfact. Det., **43**, no. 5, 2006, p. 262
9. TMAKOVA, L., SEKRETAR, S., SCHMIDT, S., Chem. Papers, **70**, no. 2, 2016, p. 188.
10. ZDZIENICKA, A., SZMCZYK, K., KRAWCZYK, J., JANCZUK, B., Fluid Phase Equilib., no. 322-323, 2012, p. 126
11. HOLMBERG, K., Curr. Opin. Colloid Interface Sci. **6**, 2001, p. 148
12. NASIRU, T., AVILA, L., LEVINE, M., J. High School Res., **1**, no. 2, 2011, p. 001
13. PATIST, A., BHAGWAT, S.S., PENFIELD, K.W., AIKENS, P., SHAH, D.O., J. Surfact. Det., **1**, no. 3, 2000, p. 53
14. SALEM, J.K., EL-NAHAL, I.M., NAJRI, B.A., HAMMAD, T.M., Chem. Phys. Lett., **664**, 2016, p. 154
15. OLTEANU, R. L., NICOLESCU, C. M., BUMBAC, M., Analytical Letters, **50(17)**, 2017, p. 2786
16. NICOLESCU, C. M., OLTEANU, R. L., BUMBAC, M., Analytical Letters, **50(17)**, 2017, p. 2802
17. RADULESCU, C., HOSSU, A.M., IONITA, I., MOATER, E.I., Dyes Pigm., **76**, no. 2, 2008, p. 366
18. RADULESCU, C., HOSSU, A.M., IONITA, I., Dyes Pigm., **71**, no. 2, 2006, p. 123
19. RADULESCU, C., TARABASANU-MIHAILA, C., Rev. Chim. (Bucharest), **57**, no. 10, 2006, p. 1034
20. RADULESCU, C., Rev. Chim. (Bucharest), **56**, no. 2, 2005, p. 151
21. RADULESCU, C., STIHI, C., POPESCU, I.V., VARATICEANU, B., TELIPAN, G., BUMBAC, M., DULAMA, I. D., BUCURICA, I. A., STIRBESCU, R., TEODORESCU, S., J. Sci. Arts, **1**, no. 34, 2016, p. 77
22. RADULESCU, C., STIHI, C., IORDACHE, S., DUNEA, D., DULAMA, I.D., Rev. Chim. (Bucharest), **68**, no. 4, 2017, p. 805
23. IORDACHE, S., DUNEA, D., IANACHE, C., RADULESCU, C., DULAMA, I.D., Rev. Chim. (Bucharest), **68**, no. 4, 2017, p. 879
24. BINTINTAN, A., GLIGOR, M., DULAMA, I.D., TEODORESCU, S., STIRBESCU, R. M., RADULESCU, C., Rev. Chim. (Bucharest), **68**, no. 4, 2017, p. 847
25. KARIMI, M.A., MOZAHEB, M.A., HATEFI-MEHRJARDI, A., TAVALLI, H., ATTARAN, A.M., SHAMSI, R., J. Anal. Sci. Tech., **6**, no. 1, 2015, p. 1
26. ZHANG, W., QIAO, X., CHEN, J., Mat. Sci. Eng. B, **142**, 2007, p. 1
27. MAY, S., BEN-SHAUL, A., J. Phys. Chem. B, **105**, no. 3, 2001, p. 630
28. WILLETS, K. A., VAN DUYNE, R. P., Annu. Rev. Phys. Chem., **58**, p. 267
29. HONG, K., TOKUNAGA, S., KAJIUCHI, T., Chemosphere, **49**, 2002, p. 379
30. KHAN, Z., AHMED AL-THABAITI, S. A., EL-MOSSALAMY, E. H., OBAID, A. Y., Colloids Surf. B Biointerfaces, **73**, 2009, p. 284
31. HENGLEIN, A., Chem. Rev., **89**, no. 8, 1989, p. 1861
32. LEWIS, L. N., Chem. Rev., **93**, no. 8, 1993, p. 2693
33. PILENI, M. P., J. Phys. Chem., **97**, no. 27, 1993, p. 6961
34. ALMUTAIRI, M. S., ALI, M., Nat. Prod. Res., **29**, no. 13, 2015, p. 1271
35. IQBAL, A., KHAN, U., SHATISTA, P., MOHAMMAD, S. A., VIQAR, U. A., Pak. J. Pharm. Sci., **7**, 1994, p. 33
36. VENU, R., RAMULU, T. S., SUNJONG, O., CHEOLGI, K., Ind. Eng. Chem. Res., **52**, 2013, p. 556
37. SHARMA, P., BABU, P. J., BORA, U., Micro & Nano Letters, **12**, no. 7, 2012, p. 1296
38. HULUBA, R., PIRVU, C., NICOLESCU, C. M., GHEORGHE, M., MINDROIU, M., Mat. Plast., **53**, no. 1, 2016, p.130
39. POPESCU, S., MINDROIU, M., CABUZU, D., PIRVU, C., Journal of Nanoparticles, 2016, p.1, <http://dx.doi.org/10.1155/2016/9747931>

Manuscript received: 7.06.2017